RESEARCH ARTICLE





Design and manufacture of a high precision personalized electron bolus device for radiation therapy

Faisal Khaled Aldawood¹ | Sha X. Chang² | Salil Desai^{1,3}

³Wake Forest Institute for Regenerative Medicine, Wake Forest School of Medicine, Winston-Salem, North Carolina

Correspondence

Salil Desai, Department of Industrial and Systems Engineering, North Carolina A&T State University, 422-B McNair Hall, 1601, East Market St., Greensboro, NC 27411,

Email: sdesai@ncat.edu

Funding information

NIH-NCTraCS. Award No. 4DR31503, NSF CMMI Award No. 1663128, Center of Excellence in Product Design and Advanced Manufacturing (NC A&T SU).

Abstract

This paper investigates a novel design and manufacturing methodology for an unmet need in radiation therapy—dose optimization of electron beam bolus. A thin-walled bolus design was proposed which when filled with water, optimized the dose distribution for the electron beam radiation therapy. The fabrication of this design was accomplished by the fused deposition modelling (FDM) additive manufacturing (3D Printing) technique. Acrylonitrile butadiene styrene (ABS) and polycarbonate (PC) materials were employed for fabricating the electron boluses. Our data show that both the materials displayed expected radiation modulation. The designed boluses were subjected to higher radiation doses (50 Gy) and revealed permissible deformations based on the dimensional deviation analysis. Mechanical deformation tests were performed to evaluate the bolus design and materials under different loading conditions. The results showed that the ABS material had superior mechanical strength and deformation behaviour as compared to PC. Finite element analysis of the bolus designs revealed regions of stress concentration and potential failure modes which were validated by experimental results. The design of experiments analysis showed that bolus thickness and material type had a profound influence on the mechanical deformation of the bolus. The proposed radiation device technology is cost-effective, eco-friendly and amenable to changes in the tumour size and shape, compared to current methods. This paper provides a framework for the design and manufacture of radiation modulation devices that can be implemented for proton, electron and photon cancer therapies.

KEYWORDS

3D printing, additive manufacturing, electron bolus, finite element analysis, medical device, radiation therapy

1 | INTRODUCTION

The Centers for Disease Control and Prevention reported that there were more than 1.5 million people in the United States suffering from cancer, and the estimated death toll was about half a million (Murphy, Kochanek, Xu, & Arias, 2015). Globally, the estimated deaths from cancer-related illness have reached about 9.6 million every year (Bray et al., 2018). The growing number of cancer patients indicates the importance of new discoveries and inventions to effectively and safely treat

cancer. Radiation therapy is a powerful and effective treatment to treat malign tumours. However, radiation can also damage normal tissues. Thus, optimizing radiation dose, such as electron beam dose, can have important impact on the quality of cancer treatment. The optimization of radiation dose distribution can be accomplished by personalized radiation modulation devices such as compensators for photon beams (Zhu et al., 2015) and bolus for electron beams (Ma et al., 2003). Using high-energy radiation, radiation therapy controls the growth of cancer cells, relieves the symptoms (Baskar, Lee, Yeo, & Yeoh, 2012)

¹Department of Industrial and Systems Engineering, North Carolina A&T State University, Greensboro, North Carolina

²Department of Radiation Oncology, UNC School of Medicine, Chapel Hill, North Carolina

and damages or shrinks the DNA in the cancer cells (DeVita, Lawrence, & Rosenberg, 2008). The art of radiation therapy is tumour eradication with minimum damage to the normal tissue. There are several customized radiation treatment devices used to achieve this goal. They include proton compensators (Trofimov & Bortfeld, 2003), photon compensators (Chang, Cullip, Deschesne, Miller, & Rosenman, 2004) and electron boluses (Hogstrom & Almond, 2006), all designed to optimize the radiation dose distribution in the cancer treatment. For electron beam therapy, customized boluses are commercially available but processing time and cost prevents its widespread application (Dotdecimal, 2019).

Computer numerical controlled (CNC) machines are commonly used to manufacture a range compensator (RC) that is prepared by the treatment planning system (TPS). However, the computerized milling machine (CMM) has limitations that includes a lower resolution of the RC device being fabricated. The TPS does not yet consider the frame of the actual drill bit, and the final fabricated device has a surface profile that appears like a chopped circular cone (Li et al., 2010). The plunged technique is another method for manufacturing radiation therapy devices and is the most common method for the fabrication of compensators. This technique mills the compensator over a chain of points by traversing them one-by-one in order to reach the specific depth and diameter. This technique involves hundreds of plunge points in order to design the compensator, which can result in higher costs and longer lead times affecting patient treatment (Tabibian et al., 2015). Due to the thickness of the shape, the plunge points usually go off-target. In addition to these limitations, a CNC machine requires a sizeable workspace and involves a complex fabrication process (Ju et al., 2014). The current fabrication technique offers a limited resolution to the compensators' profiles and requires dedicated machinists. Currently, hospitals outsource the manufacturing of radiation devices which can take between 72 hr or longer. Moreover, the CMM-based fabrication is a subtractive process that leads to larger amounts of scrap material that can harm the environment.

In recent years, the use of 3D printing technology is gaining popularity over other fabrication methods due to its simplicity of use and relatively low cost (Hwang, Zhu, Victorine, Lawrence, & Chen, 2018). Depending on the type of additive manufacturing equipment, different material can be printed such as plastic, ceramic, sand, wax and metals (Elhoone, Zhang, Anwar, & Desai, 2019; Kruth, Leu, & Nakagawa, 1998; McKenzie & Desai, 2018; Parupelli & Desai, 2017). Additive manufacturing (AM) popularly called as 3D printing can be used to fabricate radiation devices layer-by-layer with a fine resolution and at a low cost (Parupelli & Desai, 2019; Pearce et al., 2010). As compared to conventional CNC machining, 3D printing has the capability of building complex geometric profiles without specialized tooling or programming (Desai & Haeberle, 2019; Ferrando-Rocher, Herranz-Herruzo, Valero-Nogueira, & Bernardo-Clemente, 2018; Haeberle & Desai, 2019). Moreover, it is a high precision technology which can deliver a flexible treatment modality for compensators and bolus devices (Burleson, Baker, Hsia, & Xu, 2015; Zou et al., 2015). In recent years, alternative polymeric materials are being used with 3D printers over the traditional metal compensators. However, compared to a traditional 2D treatment plan, the 3D treatment plan for 3D printing

requires more complex calculations (Shafiee & Atala, 2016). Given the promise of 3D printing technology, its usage has been expedited to focus radiation on the target tumour site and minimize damage within the vicinity to healthy tissue (Bennett, 2010). In spite of the fact that 3D printing technology, in theory, can produce a dose optimizing bolus, it is challenged with non-water equivalence and density inconsistency. We propose a technology that can address these challenges.

This research aims to develop a design and manufacturing methodology for additive manufacturing (3D printing) of electron bolus devices for radiation therapy. Our team proposes the design and manufacture of a novel range compensator device that can be customized for patient requirements. We plan to augment the usage of combination media (such as water) along with a thin-walled compensator design for better radiation-beam focusing properties. The proposed method will permit high accuracy dosing of electron beams at target-specific sites within the tumour and limit adverse radiation effects to healthy tissue. This device technology will be highly amenable to changes in tumour sizes and shapes which cannot be achieved by current fabrication methods. The new design, material and process combination will cater to all the three radiation treatments (proton, electron and photon beam) with alterations to the basic design. Further, the new design will be cost-effective, eco- and user-friendly in hospital settings.

2 | METHODOLOGY

In this research, the design and manufacturing of electron bolus using additive manufacturing were implemented in four steps (Figure 1). The first step involved obtaining a computer tomography (CT) scan of the patient's tumour to determine its shape, size and location within the tissue. This was followed by developing a dosimeter algorithm to focus the radiation on the tumour site based on the CT scan. Data from the algorithm were translated into a computer-aided design (CAD) model to create a custom design for the bolus. Finally, the bolus design was fabricated using a 3D printer with different polymeric materials and tested for in-field usage.

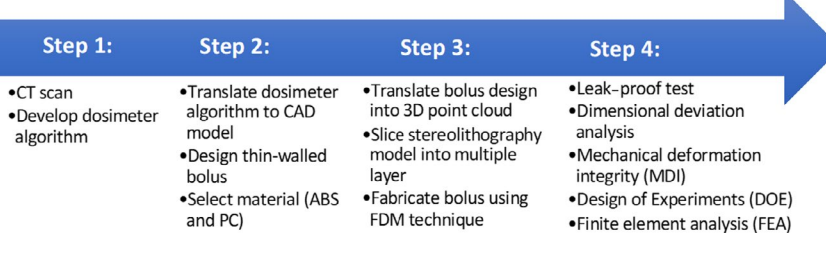
3D printing of the bolus enables the combination of a fillable media such as water along with a thin-walled bolus for better radiation-beam focusing properties. This method permits high accuracy for superior tumour coverage while minimizing the adverse radiation effects on healthy tissue. During treatment, this device technology is more amenable to changes in the tumour size and shape, compared to current methods.

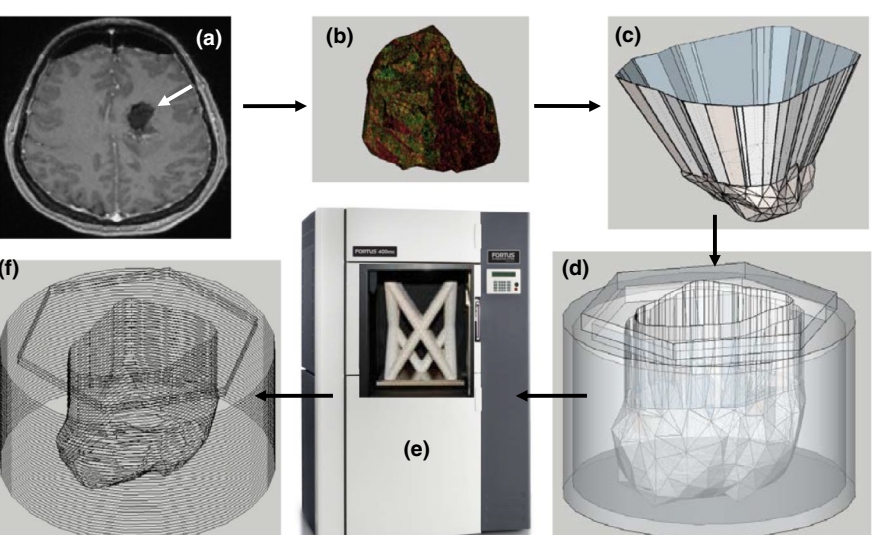
2.1 | Device design

2.1.1 | Develop a novel device design

The core innovation in this research was designing the bolus as a thinwalled hollow container which can use a recyclable fillable media such as water. The thin-wall design makes the fabrication process much

FIGURE 2 Steps to design and manufacture of electron bolus. (a) CT scan of tumour (Image credit: Dr. Tong Zhu, University of North Carolina, Chapel Hill). (b) Extraction of tumour profile. (c) Calculation of depth range data. (d) CAD design (.stl format) of hollow (bottle-like) bolus. (e) 3D printing machine. (f) Layerby-layer fabrication of the complex bolus design





faster. Compared to traditional solid system design, the thin-wall design required 80% less material usage. Further, the fillable media makes the device locally recyclable, thereby reducing the cost and carbon footprint of the process. The 3D profile of the design was extracted from depth range data calculated using a radiation planning algorithm. The liquid media (water) has consistent radiation modulation properties and fills the hollow regions of the bolus. The wall thickness and depth range data of the design can be modified to meet the requirements of different radiation therapies with adaptation to the basic design. The design of the bolus was modified by using the Autodesk MeshMixer software to create thin walls for the hollow devices. A hole formation operation (hole diameter = 5 mm) was performed to fill the boluses with water for water-equivalent electron bolus application or heavy metal granules for the intensity-modulated radiotherapy (IMRT) compensator application. Rubber (neoprene) plugs were procured to seal the hole during its usage in clinical and testing stages. The rubber plug is a quick method to seal the bolus which can be performed in a few seconds versus a screw design that needs tighter manufacturing tolerances. Moreover, the rubber plugs are cheap (\$0.25/plug) and reusable for different bolus designs. Different bolus shell thicknesses were designed ranging from 0.5 to 3 mm to test for their watertight leak-proof design.

2.1.2 **Device material**

Currently, the traditional bolus designs are manufactured using polymethyl methacrylate (PMMA) typically called (poly) for solid

piece compensators. The approach of this study was to use alternate materials with enhanced radiation modulation and strength properties. The proposed materials were acrylonitrile butadiene styrene (ABS) and polycarbonate (PC). ABS and PC materials have high strength, rigidity and material integrity characteristics (Lambert, Tang, & Rogers, 2001) that are essential for a hollow structure to maintain its shape during usage. Further, these materials display superior radiation modulation characteristics (Anbalagan, 2008) and are readily recyclable (Antonakou & Achilias, 2013; Liu & Bertilsson, 1999).

Device manufacturing method

This research employed a 3D printing technology to accurately fabricate the thin-walled bolus design (Berman, 2012; Gibson, Rosen, & Stucker, 2014). Figure 2 shows the schematic of the bolus fabrication method. The process consists of scanning the tumour dimensions (shape, size and location) using radiographic scanning such as CT or MRI (Figure 2a). Based on the radiation dosimeter profile of the electron beam (Figure 2b), the tumour dimensions are translated into a 3D profile for the compensator design (Figure 2c). Using Insight[©] 3D manufacturing software, the three-dimensional model was transformed into a point cloud to be converted into a 3D solid model. This model was exported to standard CAD software (SolidWorks) and converted into a tessellated file format (.stl). The fused deposition modelling (FDM) additive manufacturing technique (Fortus 400mc printer) was used to slice the 3D model and fabricate the bolus (Figure 2e). The FDM technique employs multiple micro-extrusion nozzles to extrude filaments of the desired material layer-by-layer on a flat platform to build the final 3D part (Figure 2f).

As compared to the conventional machining process, the 3D printing process can build highly complex geometric profiles without specialized tooling or programming. The 3D printer can be operated by lay personnel (radiation lab technicians) without the need for skilled machinist. In addition, the 3D feature and profile resolutions of additive manufacturing methods are several orders higher (microns) as compared to conventional machining (mms). It is important to note that higher resolutions can significantly benefit the radiation depth modulation within the profiles of the tumour and spare normal tissue (Kudchadker, Antolak, Morrison, Wong, & Hogstrom, 2003; Kudchadker et al., 2002). In addition, the fabrication of a hollow (bottle-like) compensator design would not be feasible by conventional machining and would need other equipment-intensive manufacturing processes such as injection moulding/blow moulding which cannot cater to small part quantities (one-off part quantity that is needed for compensator fabrication).

2.3 | Device testing

The manufactured boluses were subjected to several tests in order to validate their usability within clinical settings. The bolus was checked for any leaks due to poor fabrication as it will be carrying liquid media for radiation modulation. This was followed by a dimensional deviation analysis to evaluate its deformation pre- and postradiation exposure during therapy. Mechanical integrity tests were performed on the designed boluses with different sets of variables based on its physical handling with radiation equipment in clinical settings. Finally, a finite element analysis (FEA) was performed on bolus designs to validate its mechanical strength with the experiments. The FEA also provided guidance on both the material and process variables for customizing the design of robust boluses for radiation therapy.

2.3.1 | Leak-proof test

The boluses were designed to be filled with fillable media such as water. Thus, the boluses were tested for a leak to prevent any failure during the radiation therapy session. The boluses were filled with water and closed with a rubber plug. Boluses lesser than 1 mm thickness had crevices through which water seeped from the part. This particularly occurred due to the irregular shape of the bolus, and the layered approach to fabricating the part had a lower overlap of the material causing leaks in thinner boluses. In the case of a leak, the bolus was coated with a spray of waterproof overcoat called Clear Acrylic Sealer Gloss. Boluses with a thickness equal to or greater

than 1 mm did not have leakage problems. Thus, 1 and 3 mm boluses were considered for further tests.

2.3.2 | Dimensional deviation analysis

Variations in the bolus dimensions (x, y and z) were measured using a 3D laser scanner (Escan 2.0) and validated using Cloud Compare software. The first analysis was to compare the points of clouds for the original CAD file (.stl format) to the bolus fabricated using the 3D printer. This analysis validates that the customized boluses were fabricated precisely with accurate dimensions. In the second analysis, the boluses were compared pre- and post-exposure to substantially higher levels of radiation. This test assured that the bolus was capable to handle high radiation intensities without deforming during the therapy sessions. Dimensional changes greater than 0.3 mm (in x, y and z) and shape profile variations beyond 2% of established standards indicate unacceptable deformations of the device. In addition, a visual inspection was performed to check for material degradation and scarring of the bolus.

2.3.3 | Mechanical deformation integrity testing

Electron boluses manually undergo handling during the radiation procedure. In addition, they are subjected to bending forces within the radiation equipment. We evaluated both the bolus materials (ABS and PC) for manual handling using anthropometric data. We considered maximum finger and palm strength (80 N) when handling the electron bolus ("Human engineering design criteria for military systems, equipment and facilities," 1989). The



FIGURE 3 Mechanical deformation testing setup

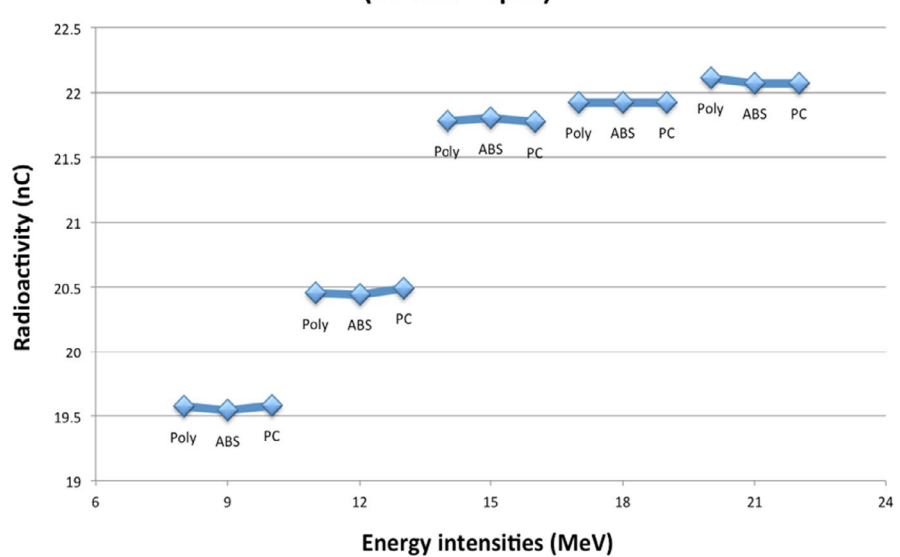
mechanical test was simulated for a typical clinical use which consisted of daily radiation exposure for 20 days. A 3-point bend flexural and a failure test (ASTM D790_10 Standard for Flexural Testing of Plastics; Specimens, 2014) were implemented using an MTS hydraulic load frame (Instron 5900 series) to evaluate shape conformance of the bolus design (Figure 3). Since the average human finger and palm grip cannot generate force beyond 80 N, the load was set at 80 N for the 3-point bend flexural. In addition, the bolus was loaded for failure test in order to determine the load and deformation that a bolus can endure before cracking. Figure 3 shows the 3-point bending fixture and test specimen. Load cells were attached to the setup to record the deformation displacement at the centre point as the load was increased. A sample size of eight devices (n = 8) for each material (ABS and PC) with different thicknesses (1 and 3 mm) and manufacturing

orientations (horizontal and vertical) was used to test the bolus. The StrainSmart[®] data acquisition software was used to read the deformation values of the bolus.

2.3.4 | Design of experiments for the mechanical deformation test

A design of experiments was conducted in order to evaluate the effect of four input factors (k = 4) on the output response at two levels using a 2^4 full factorial design. The factors include the following: A: design (thin wall—1 mm and thick wall—3 mm); B: material type (ABS and PC); C: manufacturing orientation (vertical and horizontal); and D: force (50 and 110 N) on the response variable (maximum deformation displacement). The response variable values were obtained from the results of

(a) Radiation dosages at different energy intensities (10 mm depth)



(b) Radiation dosages at different energy intensities (30 mm depth)

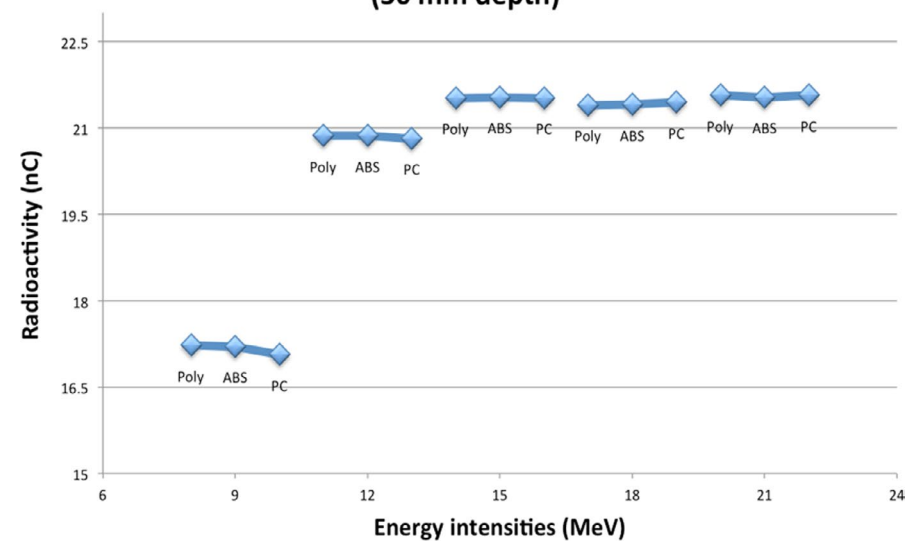
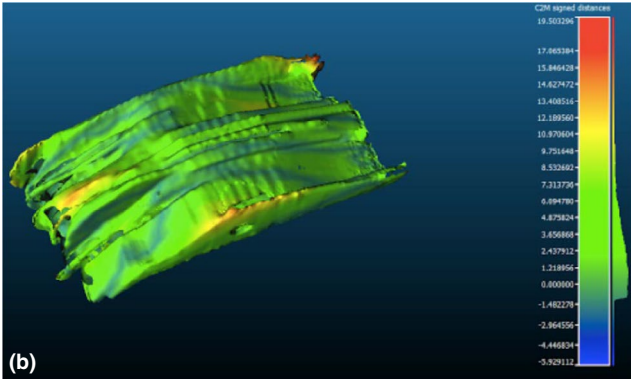


FIGURE 4 (a) Radioactivity results of Poly, ABS and PC (10 mm depth). (b) Radioactivity results of Poly, ABS and PC (30 mm depth)





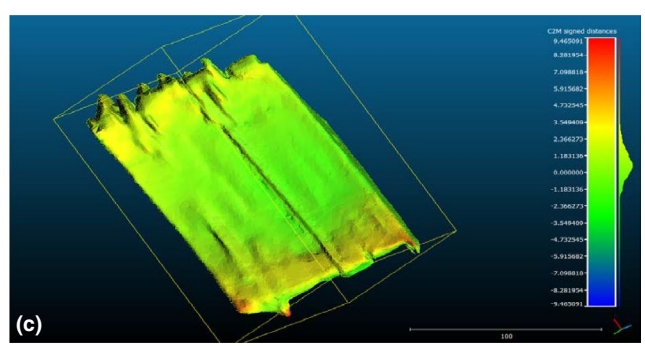


FIGURE 5 (a) 3D dimensional deviation analysis scanning setup. (b) Dimensional deviation analysis of PC bolus after fabrication. (c) Dimensional deviation analysis of PC bolus after exposure to radiation

the mechanical deformation tests. ANOVA was used to analyse the results of the design of experiments at α = 0.05.

2.3.5 | Finite elements analysis of bolus

A finite element analysis (FEA) was conducted on the electron boluses for different materials, thicknesses and loads using Abaqus software. The bolus was loaded with identical loading and boundary conditions as per the mechanical bending test. The top of the bolus was loaded with 80 N compressive load, and the bottom regions of the bolus were supported for fixed boundary conditions (Ux, Uy, Uz = 0). Appropriate material properties were inputted to the FEA model with a factor to account for non-homogeneous material based on the layered 3D part. The material properties for ABS material included Young's modulus of 1.44e9 Pa and a Poisson rate of 0.35. Similarly, the PC material had Young's modulus of 1.37e9 Pa and a Poisson ratio of 0.37. A tetrahedral mesh element was used with an

aspect ratio of 1.5 to accommodate intricate geometries within the bolus. Von Mises stress values were calculated to evaluate the bolus design. The FEA models were validated with results from the experimental runs for the mechanical tests.

3 | RESULTS AND DISCUSSION

3.1 | Material validation test

The chosen materials for the electron bolus (ABS and PC) were tested for radiation modulation properties. These materials were compared with polymethyl methacrylate (poly) which is the standard material used for fabricating electron boluses using CNC milling machines. Figure 4a,b shows the radiation modulation properties for ABS and PC as compared to poly for different intensities of radiation. A (10 mm × 10 mm × 2 mm) sheet was fabricated using 3D printing of ABS and PC materials. These sheets were tested for radiation dosage equivalency using a sensor that measures the dosage of radiation at a depth of 10 and 30 mm, respectively. The vertical axis is the radiation measurement ion chamber reading that is proportional to the dose. The test pieces were subjected to different radiation intensities (9-21 MeV) to observe their effect on the radiation equivalency with the poly material. As can be seen from the graphs in Figure 4, both ABS and PC materials had equivalent properties as the PMMA (poly) for different radiation intensities. This experiment validated the fact that the new materials being considered for fabricating the electron bolus had equivalent radiation modulation properties. This finding is important as the radiation planning software does not need to be adjusted to accommodate for the new materials.

3.2 | Radiation exposure

The electron boluses were irradiated at 50 Gy to test the integrity of the bolus device under radiation. The clinical dose level is in the range of 10–20 Gy. An 18 MeV electron beam was used on a Siemens Artiste linear accelerator. The boluses were irradiated using a 20×20 -cm electron cone. The deformation behaviour of the bolus showed no significant impact after exposure to a high dosage of radiation as confirmed by the dimensional deviation analysis.

3.3 | Dimensional deviation analysis

The 3D-printed boluses were scanned for both ABS and PC materials (n=5 for each material) for determining their dimensional deviation from the original CAD (.stl file). Multiple images (>60 images per bolus) were scanned at 10-degree intervals in orthogonal axes to create a composite 3D point cloud file (Figure 5a). After scanning the 3D-printed boluses, a point cloud was generated and compared with the point cloud of the original CAD file. The cloud-to-cloud difference between the

original STL file and scanned 3D-printed bolus had a mean deviation distance of 0.12 mm and a standard deviation of 0.57 mm (Figure 5b). The point clouds for the original CAD file and fabricated boluses were within the prescribed threshold to conclude that the additively manufactured bolus had precise dimensions for radiation therapy.

The second dimensional deviation analysis was performed for pre- and post-radiation of the boluses (n = 5 for each material type). Figure 5c shows that there were no significant differences in the geometry of the bolus pre- and post-exposure to radiation. The mean deviation distance in this comparison was about 0.15 mm, and the standard deviation was 0.32 mm. The overall shape difference between pre- and post-radiation was 0.43% which is within the acceptable limit of 2% shape variation. These results emphasize that the bolus maintained its dimensional and shape integrity during the radiation session despite exposure to high radiation beams. Thus, it could be used multiple times for several radiation sessions.

3.4 | Mechanical deformation integrity testing

Table 1 shows the deformation and load levels exerted on the bolus designs for different materials and thicknesses. The bolus was tested for a load of 80 N, which is the average force generated during a human grip (Standard, 1989). In addition, the bolus was loaded through failure for both vertical and horizontal manufacturing build orientations. As seen in Table 1, ABS material displayed higher strength as compared to PC material for all the loading scenarios. The typical force to failure for ABS was higher >200 N as compared to PC for 1 mm thickness bolus in both orientations. Similarly, the load to failure was greater in ABS >950 N as compared to PC (around 500 N) for the 3 mm thickness bolus. For both the materials with the bolus thickness of 1 mm, the

vertical orientation had higher deformation at failure and subsequently lower bolus strength as compared to the horizontal orientation. This can be attributed to the fact that the vertical fabrication orientation was parallel to the loading direction, thereby offering lower resistance to deformation. The vertical direction of fabrication caused slippage and deformation of the 3D-printed layers as the load increased to failure. The 3 mm boluses had lower deformation and higher strength as compared to the 1 mm boluses based on the increased cross-sectional area. These findings were consistent for both the ABS and the PC boluses. Similarly, ABS boluses observed lower deformation as compared to PC boluses which were consistent with their loading behaviour as explained above. The ABS bolus displayed an elastic deformation behaviour (Figure 6a) with minor cracks in the bolus device. The ABS bolus with 1 mm thickness deformed until failure for both fabrication orientations and recovered its shape after release of the load (closed loop curve). A similar recovery trend is observed for the 3 mm bolus with horizontal fabrication orientation. However, the 3 mm bolus with vertical orientation had significant cracks and did not recover its original shape (open deformation curve).

Figure 6b shows that the PC boluses were fractured at failure loads due to its brittle nature. ABS bolus deforms and induces both elastic and plastic deformation, whereas PC material is brittle and cracks when subjected to higher loads without yielding as seen from Figure 6a,b, respectively. Figure 6b shows that all boluses cracked when loaded to failure and did not recover the original shape. The 3 mm PC bolus with horizontal fabrication orientation was able to recover its shape due to higher cross-sectional area and perpendicular build orientation with respect to the loading direction. The mechanical deformation integrity test results revealed that the designed boluses were capable of performing their intended function without any significant deformation during radiation therapy.

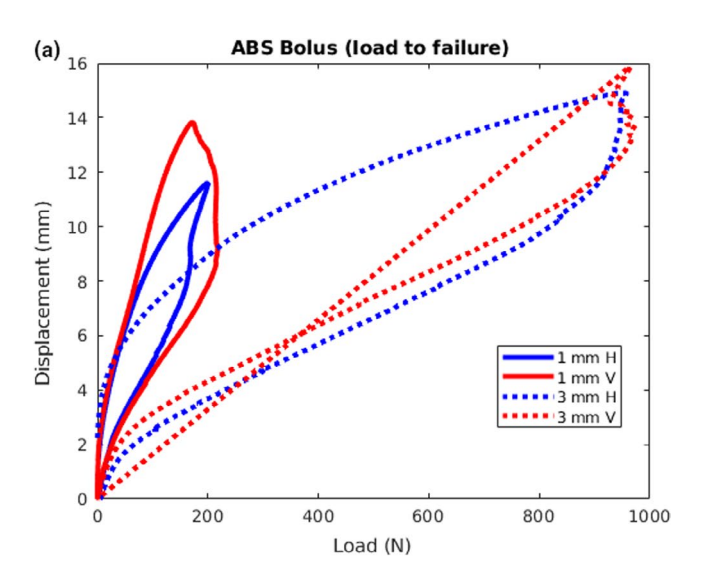
TABLE 1 Mechanical deformation integrity test results

Material	Thickness (mm)	Maximum load (N)	Manufacturing orientation	Maximum displacement (mm)
ABS	1	80	Horizontal	4.123
		Failure (200)		11.589
		80	Vertical	3.374
		Failure (217)		13.817
	3	80	Horizontal	2.162
		Failure (957)		14.902
		80	Vertical	2.930
		Failure (974)		15.879
PC	1	80	Horizontal	6.862
		Failure (110)		9.714
		80	Vertical	5.587
		Failure (144)		9.714
	3	80	Horizontal	3.024
		Failure (489)		8.087
		80	Vertical	3.345
		Failure (533)		8.467

However, the ABS material is the preferred choice for fabricating the boluses based on their deformation behaviour and mechanical properties.

3.5 | Design of experiments of the mechanical deformation integrity test

A design of experiments was performed to evaluate the bolus design based on interactions between four different factors which include



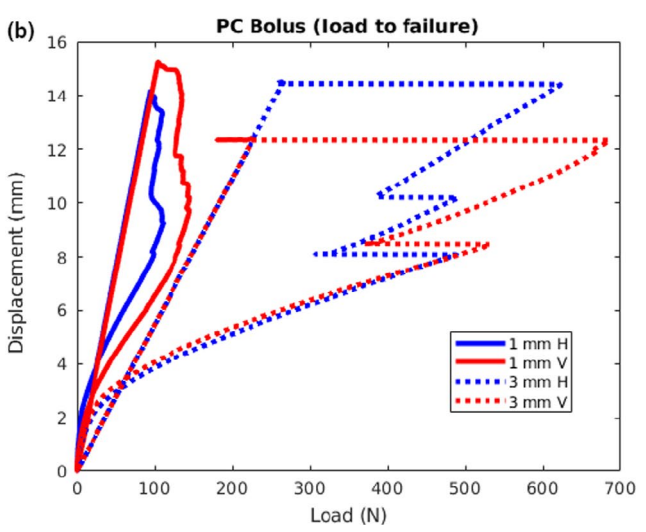


FIGURE 6 (a) Load-displacement curve for ABS bolus. (b) Load-

material type, bolus thickness, loading force and fabrication orientation. Table 2 shows the ANOVA results (α = 0.05). Based on the p-values, it is clear that the bolus thickness, loading force and material type were the significant factors in this experiment. Figure 7a also shows that the thickness of the bolus is the most significant factor affecting its deformation behaviour, followed by materials type and loading force. Figure 7b shows the main effect plot for the mean maximum displacement for the different factors considered. Increasing the thickness of the bolus wall will reduce the maximum displacement (inverse relationship). Moreover, the loading force had a direct relationship with the deformation. The bolus thickness showed differences in the mean displacement between 5.4 mm for the 1 mm thickness and 3 mm for the 3 mm bolus thickness, respectively. Significant differences in mean displacement were observed between ABS and PC materials. Similar trends were observed for the force levels of 50 and 100 N. However, the manufacturing orientation had a marginal effect on the displacement between horizontal and vertical orientation in designing the boluses.

3.6 | Finite element analysis

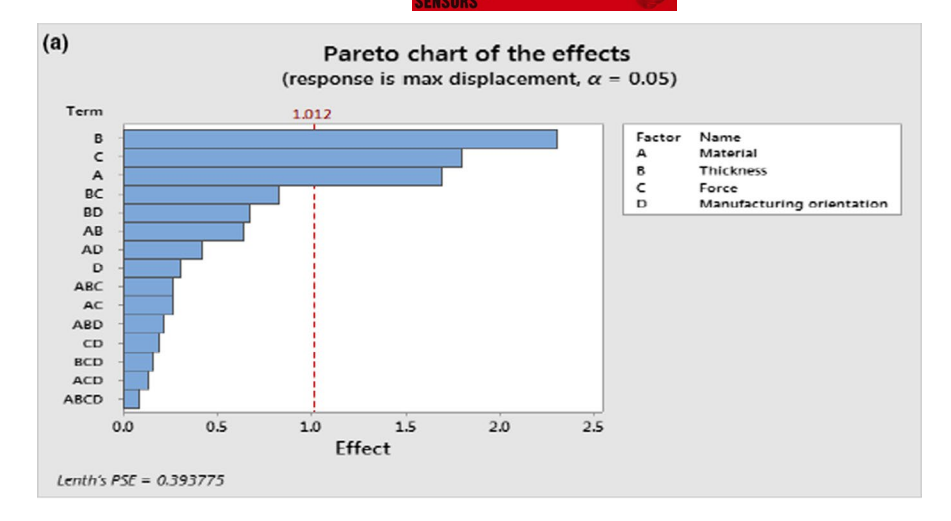
Finite element analysis was conducted to evaluate both the deformation behaviour and von Mises stresses in the boluses (scale shown in Figure 8 are in SI units). Figure 8a shows that the maximum deformation of the ABS bolus was located at the top centre of the bolus at the point of loading. The maximum displacement value for the ABS bolus with 1 mm thickness was 3.813 mm (units shown in Figure 8a are in metres) for a load of 80 N which was validated by the experimental results (range between 3.3-4.123 mm). The maximum von Mises stress was concentrated at the point of loading with a value of 7.52e7 Pa (units shown in Figure 8b are in Newton per square metres) leading to stress concentration as shown in Figure 8b. Figure 8c shows that the bolus tested experimentally at higher failure loads fractured at this point thereby confirming the validity of the FEA model. Similarly, PC bolus with 1 mm thickness exhibited a maximum displacement of 6.23 mm and maximum von Mises stress of 9.93e07 Pa for a load of 80 N. It is evident that the ABS bolus had lower displacement and von Mises stress values as compared to the PC bolus thereby confirming the findings from the experimental results. The FEA results provided insight into capturing the deformation and failure behaviour of the boluses without the need to run large-scale experiments that consume resources and time. In addition, they

Source	df	Seq SS.	Adj SS	Adj MS	F	р
Material	1	10.726	10.726	10.726	12.26	.005
Thickness	1	19.693	19.693	19.693	22.52	.001
Force	1	17.895	17.895	17.895	20.46	.001
Manufacturing orientation	1	0.422	0.422	0.422	0.48	.502
Error	11	9.620	9.620	0.875		
Total	15	58.356				

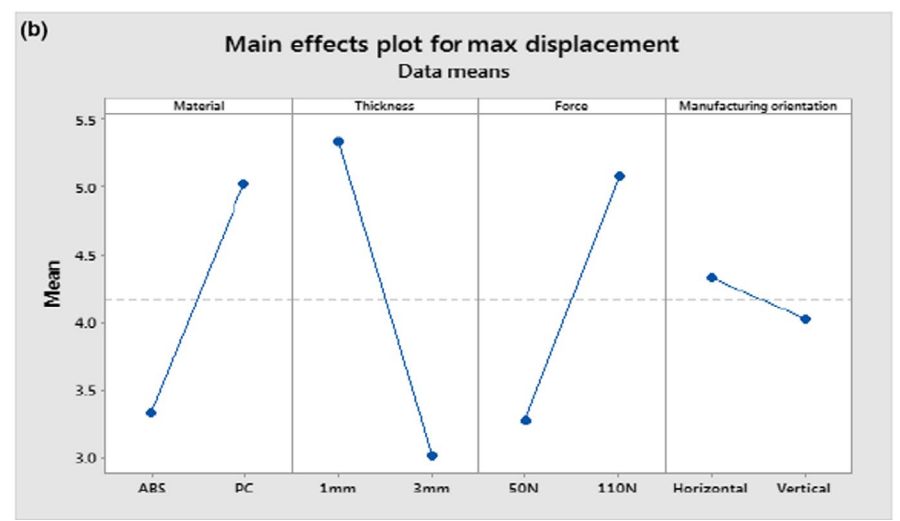
TABLE 2 Analysis of variance for maximum displacement

-WILEY 9 of 12

FIGURE 7 (a) Pareto chart of the effects for maximum displacement. (b) Main effects plot for maximum displacement



ጺ



provided a predictive tool for estimating the bolus strength for a variety of material and thickness combinations.

3.7 | Impact on radiation therapy

The proposed design and manufacturing approach for bolus and compensator devices may significantly impact radiation therapy using photon, electron and proton beams. Table 3 shows the comparative analysis of traditional versus the new approach. The new design will lead to higher accuracy dosing of malignant tissue (micron level) as compared to conventional design (mm level). This improvement will spare the healthy tissue within the proximity leading to better patient outcomes and minimize radiation side effects. The use of hollow (bottle-like) design has several advantages over solid material 3D printing design, which include the following: (a) substantial material savings (80% less material usage) and, thus, increasing the affordability of radiation treatment, (b) significantly reduced 3D printing time and (c) water equivalence of the devices, which is important for the accuracy of dose computation. The latter is important as the 3D printing materials are not water equivalent, and the

resulting density of the 3D-printed device can vary and thus introduce dose error. The ability to build customized compensator designs in-house will lead to reductions in order lead times (48–72 hr in conventional manufacturing versus 5 hr for in-house fabrication) and the elimination of transportation costs. We envision that the benefits of a better treatment modality and low-cost radiation therapy device will translate to substantial cost savings to the US medical/health care industry.

4 | CONCLUSIONS

This research investigated a novel design and manufacturing methodology for radiation modulation devices. The core innovation in this study was the 3D printing (additive manufacturing) of a thinwalled hollow electron bolus device that can accommodate fillable media such as high-Z material. A dosimeter algorithm was developed based on the CT scan and translated into a thin-walled bolus design. Acrylonitrile butadiene styrene (ABS) and polycarbonate (PC) materials displayed radiation modulation properties at different energy intensities (9–21 MeV). The fused deposition modelling (FDM)

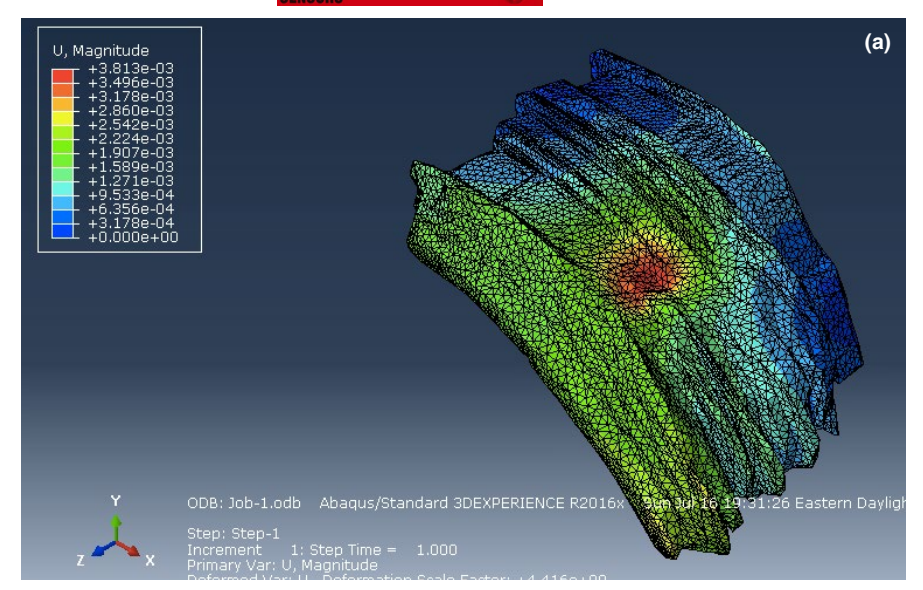


FIGURE 8 (a) Deformation behaviour of electron bolus after finite element analysis. (b) von Mises stresses for ABS bolus. (c) Fractured bolus after experimental tests

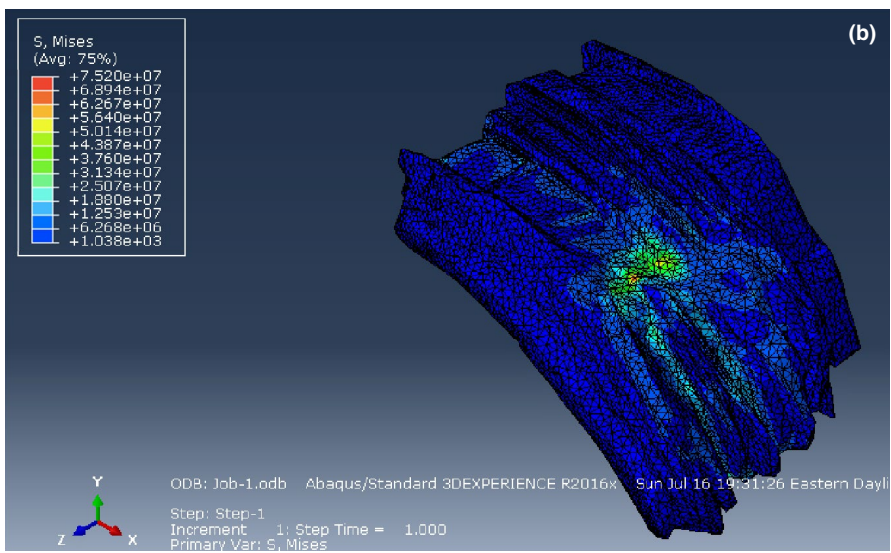




TABLE 3 Comparative benefits of new compensator design versus traditional design

Criterion	Traditional compensator	New compensator
Radiation dosage	Lower precision (mm resolution)	Higher precision (μm resolution)
Fabrication cost	High due to expensive equipment and dedicated machinist (\$1,000+)	Low-cost user-friendly 3D printing (\$100–\$150)
Manufacture turnaround	Outsourced: 48–72 hr	In-house: 5–10 hr
Environmental impact	High due to higher material usage	Environmentally friendly due to thin-walled design (80% less material)

technique was used to fabricate the boluses with 1 and 3 mm thicknesses, respectively. Dimensional deviation analysis pre- and post-radiation exposure session displayed minimal deformation (<2%) in the boluses. Mechanical deformation tests showed that the ABS bolus was superior in strength and fracture behaviour under different loading conditions. Design of experiments revealed that bolus thickness and material were significant factors (α = 0.05) that affected the deformation behaviour. The vertical manufacturing orientation during 3D printing resulted in lower strength due to the layered structure of the bolus. Finite element analysis validated the experimental testing to identify regions of stress concentration and failure when the boluses were loaded. The ABS bolus when loaded at the normal gripping force of 80 N had a maximum displacement of 3.813 mm and maximum von Mises stress of 7.52e7 Pa as compared to 6.23 mm and 9.93e7 Pa, respectively, for the PC material. This research establishes a foundation for the design and manufacture of electron bolus devices with higher precision, lower material and cost for radiation therapy.

ACKNOWLEDGEMENTS

The authors extend their gratitude to the NIH-NCTraCs. Award No. 4DR31503, National Science Foundation (NSF CMMI Award: 1663128) and the Center of Excellence in Product Design and Advanced Manufacturing (NC A&T SU) for support towards this research. We would also like to thank Dr. Tong Zhu—Dept. Radiation Oncology, University of North Carolina at Chapel Hill for providing computer tomography images of the tumours).

REFERENCES

- Anbalagan, P. (2008). Radiation damage of polymers in ultrasonic fields. International Nuclear Information System, 40(15), 4–6.
- Antonakou, E. V., & Achilias, D. S. (2013). Recent advances in polycarbonate recycling: A review of degradation methods and their mechanisms. *Waste and Biomass Valorization*, 4(1), 9–21. https://doi.org/10.1007/s12649-012-9159-x
- Baskar, R., Lee, K. A., Yeo, R., & Yeoh, K. W. (2012). Cancer and radiation therapy: Current advances and future directions. *International Journal of Medical Sciences*, 9(3), 193–199. https://doi.org/10.7150/ijms.3635
- Bennett, J. T. (2010). A feasibility study of two alternate proton radiation compensator designs for use in proton radiation therapy. Cullowhee, NC: Western Carolina University.
- Berman, B. (2012). 3-D printing: The new industrial revolution. *Business Horizons*, 55, 155–162. https://doi.org/10.1016/j.bushor.2011.11.003

- Bray, F., Ferlay, J., Soerjomataram, I., Siegel, R. L., Torre, L. A., & Jemal, A. (2018). Global cancer statistics 2018: GLOBOCAN estimates of incidence and mortality worldwide for 36 cancers in 185 countries. CA: A Cancer Journal for Clinicians, 68(6), 394–424. https://doi.org/10.3322/caac.21492
- Burleson, S., Baker, J., Hsia, A. T., & Xu, Z. (2015). Use of 3D printers to create a patient-specific 3D bolus for external beam therapy. *Journal of Applied Clinical Medical Physics*, 16(3), 166–178. https://doi.org/10.1120/jacmp.v16i3.5247
- Chang, S. X., Cullip, T. J., Deschesne, K. M., Miller, E. P., & Rosenman, J. G. (2004). Compensators: An alternative IMRT delivery technique. Journal of Applied Clinical Medical Physics, 5(3), 15–36.
- Desai, S., & Haeberle, G. (2019). Additive manufacturing (3D printing) of thermoform tooling. *International Journal of Mechanical and Production Engineering*, 7(3), 1-4.
- DeVita, V. T., Lawrence, T. S., & Rosenberg, S. A. (2008). DeVita, Hellman, and Rosenberg's cancer: Principles & practice of oncology. Philadelphia, PA: Lippincott Williams & Wilkins.
- Dotdecimal (2019). Retrieved from https://dotdecimal.com/
- Elhoone, H., Zhang, T., Anwar, M., & Desai, S. (2019). Cyber based design for additive manufacturing using artificial neural networks for industry 4.0. *International Journal of Production Research*, 1–5. https://doi.org/10.1080/00207543.2019.1671627
- Ferrando-Rocher, M., Herranz-Herruzo, J. I., Valero-Nogueira, A., & Bernardo-Clemente, B. (2018). Performance assessment of gap-waveguide array antennas: CNC milling versus three-dimensional printing. *IEEE Antennas and Wireless Propagation Letters*, 17(11), 2056–2060. https://doi.org/10.1109/LAWP.2018.2833740
- Gibson, I., Rosen, D. W., & Stucker, B. (2014). Additive manufacturing technologies (Vol. 17). New York, NY: Springer.
- Haeberle, G., & Desai, S. (2019). Investigating rapid thermoform tooling via additive manufacturing (3D Printing). *American Journal of Applied Sciences*, 16, 238–243. https://doi.org/10.3844/ajassp.2019
- Hogstrom, K. R., & Almond, P. R. (2006). Review of electron beam therapy physics. *Physics in Medicine and Biology*, 51(13), R455.
- (1989). Human engineering design criteria for military systems, equipment and facilities. US Department of Defense.
- Hwang, H. H., Zhu, W., Victorine, G., Lawrence, N., & Chen, S. (2018). 3D-printing of functional biomedical microdevices via light- and extrusion-based approaches. *Small Methods*, 2(2), 3–5.
- Ju, S. G., Kim, M. K., Hong, C.-S., Kim, J. S., Han, Y., Choi, D. H., ... Lee, S. B. (2014). New technique for developing a proton range compensator with use of a 3-dimensional printer. *International Journal of Radiation Oncology Biology Physics*, 88(2), 453–458. https://doi.org/10.1016/j.ijrobp.2013.10.024
- Kruth, J. P., Leu, M. C., & Nakagawa, T. (1998). Progress in additive manufacturing and rapid prototyping. CIRP Annals, 47, 525–540. https://doi.org/10.1016/S0007-8506(07)63240-5
- Kudchadker, R. J., Antolak, J. A., Morrison, W. H., Wong, P. F., & Hogstrom, K. R. (2003). Utilization of custom electron bolus in head

- and neck radiotherapy. *Journal of Applied Clinical Medical Physics*, 4(4), 321–333. https://doi.org/10.1120/jacmp.v4i4.2503
- Kudchadker, R. J., Hogstrom, K. R., Garden, A. S., McNeese, M. D., Boyd, R. A., & Antolak, J. A. (2002). Electron conformal radiotherapy using bolus and intensity modulation. *International Journal of Radiation Oncology Biology Physics*, 53, 1023–1037. https://doi.org/10.1016/ S0360-3016(02)02811-0
- Lambert, B. J., Tang, F. W., & Rogers, W. J. (2001). Polymers in medical applications (Vol. 127). Shrewsbury, UK: iSmithers Rapra Publishing.
- Li, H., Zhang, L., Dong, L., Sahoo, N., Gillin, M. T., & Zhu, X. R. (2010). A CT-based software tool for evaluating compensator quality in passively scattered proton therapy. *Physics in Medicine and Biology*, 55(22), 6759–6771. https://doi.org/10.1088/0031-9155/55/22/010
- Liu, X., & Bertilsson, H. (1999). Recycling of ABS and ABS/PC blends. *Journal of Applied Polymer Science*, 74(3), 510–515. https://doi.org/10.1002/(SICI)1097-4628(19991017)74:3<510:AID-APP5>3.0.CO;2-6
- Ma, C. M., Ding, M., Li, J. S., Lee, M. C., Pawlicki, T., & Deng, J. (2003). A comparative dosimetric study on tangential photon beams, intensity-modulated radiation therapy (IMRT) and modulated electron radiotherapy (MERT) for breast cancer treatment. *Physics in Medicine* and Biology, 48(7), 909.
- McKenzie, J., & Desai, S. (2018). Investigating sintering mechanisms for additive manufacturing of conductive traces. *American Journal of Engineering and Applied Sciences*, 11(2), 652–662. https://doi.org/10.3844/ajeassp.2018.652.662
- Murphy, S. L., Kochanek, K. D., Xu, J., & Arias, E. (2015). Mortality in the United States, 2014. NCHS Data Brief, 229, 1–8.
- Parupelli, S. K., & Desai, S. (2017). Understanding hybrid additive manufacturing of functional devices. American Journal of Engineering and Applied Sciences, 10(1), 264–271. https://doi.org/10.3844/ajeas sp.2017.264.271
- Parupelli, S. K., & Desai, S. (2019). A comprehensive review of additive manufacturing (3D printing): Processes, applications and future potential. *American Journal of Engineering and Applied Science*, 16, 244–272. https://doi.org/10.3844/ajassp.2019.244.272
- Pearce, J., Zelenika-Zovko, I., Blair, C., Laciak, K., Andrews, R., & Nosrat, A. (2010). 3-D printing of open source appropriate technologies

- for self-directed sustainable development. *Journal of Sustainable Development*, 3(4), 2–3. https://doi.org/10.5539/jsd.v3n4p17
- Shafiee, A., & Atala, A. (2016). Printing Technologies for medical applications. *Trends in Molecular Medicine*, 22, 254–265. https://doi.org/10.1016/j.molmed.2016.01.003
- Specimens, P. E. M. (2014). Standard test methods for flexural properties of unreinforced and reinforced plastics and electrical insulating materials. West Conshohocken, PA: ASTM International. https://doi.org/10.1520/D0790-10
- Standard, M. (1989). Human engineering design criteria for military systems, equipment and facilities. US Department of Defense.
- Tabibian, A. A., Powers, A., Dolormente, K., Oommen, S., Tiwari, A., Palmer, M., ... Nguyen, B.-N. (2015). Is there a clinical benefit with a smooth compensator design compared with a plunged compensator design for passive scattered protons? *Medical Dosimetry*, 40(1), 37–43. https://doi.org/10.1016/j.meddos.2014.07.004
- Trofimov, A., & Bortfeld, T. (2003). Optimization of beam parameters and treatment planning for intensity modulated proton therapy. *Technology in Cancer Research and Treatment*, 2(5), 437–444.
- Zhu, X., Driewer, J., Li, S., Verma, V., Lei, Y., Zhang, M., ... Wang, A. Z. (2015). Fabricating Cerrobend grids with 3D printing for spatially modulated radiation therapy: A feasibility study. *Medical Physics*, 42(11), 6269–6273.
- Zou, W., Fisher, T., Zhang, M., Kim, L., Chen, T., Narra, V., ... Ning, Y. J. (2015). Potential of 3D printing technologies for fabrication of electron bolus and proton compensators. *Journal of Applied Clinical Medical Physics*, 16(3), 90–98. https://doi.org/10.1120/jacmp. v16i3.4959

How to cite this article: Aldawood FK, Chang SX, Desai S. Design and manufacture of a high precision personalized electron bolus device for radiation therapy. *Med Devices Sens.* 2020;00:e10077. https://doi.org/10.1002/mds3.10077